Power Electronic Systems
Laboratory

Proceedings of the 14th IEEE International Power Electronics and Motion Control Conference (ECCE Europe 2011), Birmingham, UK, August 30 - September 1, 2011.

High Efficiency Drive System with 3-Level T-Type Inverter

M. Schweizer
J.W. Kolar

Eidgenössische Technische Hochschule Zürich
Swiss Federal Institute of Technology Zurich

High efficiency drive system with 3-level T-type inverter

Mario Schweizer and Johann W. Kolar
Power Electronic Systems Laboratory, ETH Zurich
Physikstrasse 3, 8092 Zurich
Switzerland
Phone: +41 44 632 27 80
Fax: +41 44 632 12 12
Email: schweizer@lem.ee.ethz.ch
URL: http://www.pes.ee.ethz.ch

Acknowledgments

The authors would like to thank Koji Kato for layouting the T-type converter and Thomas Friedli for his help with the machine test bench.

Keywords

<<Multilevel converters>>, <<Efficiency>>, <<Electrical drive>>, <<Induction motor>>, <<Converter machine interactions>>.

Abstract

In this paper an efficiency optimized variable speed drive is presented. It consists of the alternative 3-level T-type converter topology which is very efficient for low switching frequencies and a standard induction machine. The total system efficiency is optimized concerning the converter losses as well as fundamental and harmonic induction machine losses.

1 Introduction

Variable speed drives for low-voltage applications are traditionally built with 2-level inverters because of the tremendous cost pressure. Although it was shown previously that 3-level topologies offer various advantages in terms of output voltage quality, harmonic losses in the machine, isolation stress and overvoltages due to long motor cables, they have never achieved a large market penetration. The main reasons for the small acceptance are the increased costs due to the additional semiconductors, the additional gate drive units and the potentially lower reliability.

To overcome the mentioned drawbacks and still benefit from the superior 3-level voltage waveform, the alternative 3-level T-type converter ($3LT^2C$) [1–4] is considered for low-voltage variable speed drive applications. There, the conventional 2-level VSC topology is extended with an active, bidirectional switch to the DC-link mid-point as depicted in Fig. 2.

The $3LT^2C$ has several advantages compared with alternative 3-level topologies such as the well known 3-level NPC [5] or the recently presented 3-level split inductor converter [6]. Contrary to the NPC topology, the $3LT^2C$ is very efficient for low switching frequencies due to low conduction losses and needs only three additional isolated gate drive power supplies compared to the 2-level converter. Differently, the split inductor converter is able to generate 3-level voltage outputs without additional semiconductors and gate drives, but it employs bulky and expensive bridge leg inductors which also produce losses.

The $3LT^2C$ basically combines the advantages of the 2-level converter such as low conduction losses and small part count with the advantages of the 3-level converter such as low switching losses and superior output voltage quality.

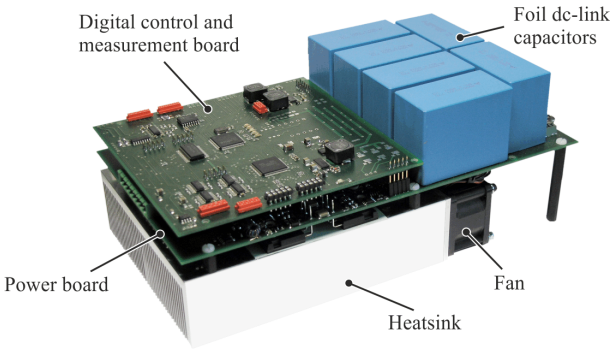

Figure 1: Prototype of the 3LT²C.

If the total drive efficiency is considered, the main share of the losses occurs in the induction machine. Several efficiency optimal machine control algorithms have been proposed in the past such as search algorithms [7] and model-based efficiency optimizers [8]. In this paper the machine will be optimally controlled with a model-based approach.

Harmonic iron and harmonic ohmic losses due to the pulsed converter output voltage can increase the induction machine losses [9]. Not only the direct losses due to the harmonics but also the change in the fundamental operating point due to the additional heating is important and influences the efficiency negatively [10].

In section 2, the 3LT²C losses and efficiency depending on the operating points of the machine are calculated and compared to the performance of the standard 2-level VSC. In section 3, the induction machine efficiency with loss minimizing control is considered. The difference of the harmonic losses caused by the 2-level and the 3-level converter is analyzed in section 4 and proved with detailed measurements on a machine test bench including a precise torque transducer. The impact of the efficiency optimal machine control on the converter operating points is analyzed and the total drive efficiency is calculated in section 5.

2 The 3LT²C prototype

2.1 Hardware setup

The 3LT²C prototype shown in Fig. 1 is implemented with 1200 V, 40 A IGBTs with antiparallel diodes (Infineon IKW40T120) forming the six-switch inverter circuit, and with 600 V, 50 A devices (Infineon IKW50N60T) for the three bidirectional switches between the phase outputs and the DC-link midpoint. Only 3 additional isolated gate drive power supplies are necessary compared to the simple 2-level converter because of the common emitter configuration of the 600 V IGBTs. Therefore, the costs can be kept low and are not comparable to the 3-level NPC topology.

The key performance data of the 3LT²C prototype is summarized in Tab. I. The converter is designed for an output power of 10 kW and allows the switching frequency to be set in a range from $4 - 24$ kHz. At the nominal switching frequency of 8 kHz, the converter reaches a pure semiconductor efficiency of 99 %. Digital control, gate drive circuits and forced air cooling consume 20 W in addition. The power density is given with 3.3 kW/dm^3.

An important feature is the ability to change the switching frequency during operation. Also the output voltage can be switched between 2-level and 3-level modulation during operation what allows an investigation of the impact on the induction machine efficiency without stopping the machine and changing its thermal conditions.

2.2 Switch commutation and modulation

The current commutation for each switching transition was considered in detail for the 3LT²C in [11]. Basically, the T-type bridge-leg can be connected to the positive, the neutral or the negative DC-link voltage level. During a switching transition the current naturally commutates to the correct branch if the 4 switches in a bridge leg are controlled in a way similar to the 3-level NPC converter [11]. It is not necessary to employ a current dependent commutation scheme, a simple turn-on delay is sufficient to guarantee reliable operation.

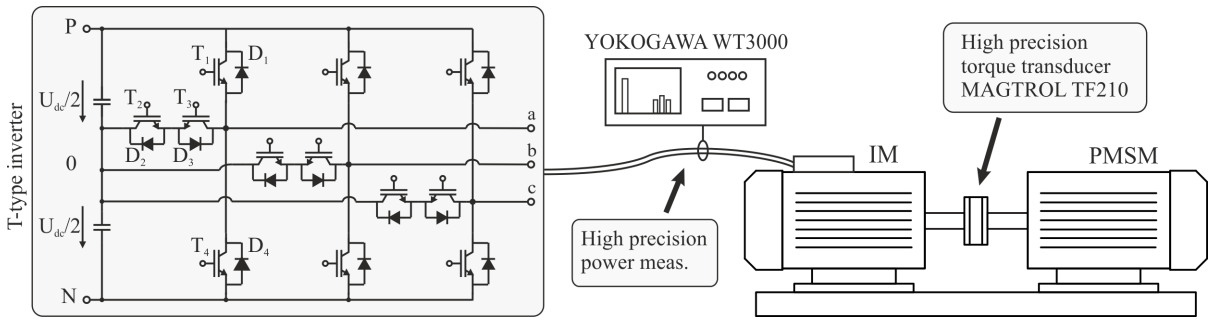

Figure 2: Schematic of the 3LT²C and the machine test bench. The graphical alignement of the top and bottom switches together with the two middle switches resemble the rotated character T. Therefore, the topology is referred to as T-type topology.

Table I: Parameters of the 3LT²C.

Parameter	Variable	Value
Nominal output power	P_n	10 kW
Nominal efficiency	η_n	99.0 %
Switching frequency	f_s	8 kHz
DC-link voltage	U_dc	650 V
DC-link capacitance	C_dc	$2 \times 240\,\mu$F in series
Volume	V	3 dm^3
Weight	m	2 kg
Power density	ρ	3.3 kW/dm^3
Power weight	σ	5 kW/kg

The modulation strategies known from the 3-level NPC converter can also be applied to the 3LT²C. The modulation strategy is an important point for the converter efficiency [12]. A space vector modulation scheme with optimal clamping described in [13] is used for the prototype. A fixed optimal clamping scheme reducing the switching losses for an inductive current displacement of 30° is implemented which best fits the induction machine terminal behavior.

An issue related to the adopted optimal clamping space vector modulation is that the DC-link capacitors are loaded in an alternating fashion with three times the fundamental frequency. Therefore a certain DC-link voltage unbalance occurs periodically and has to be explicitly allowed. The space vector modulation is adopted to account for this voltage unbalance according to [14]. The compensation ensures that the output voltage is generated correctly although the link is not exactly balanced.

2.3 Converter losses and efficiency calculation

Especially the switching losses are considerably influenced by the combination of the two switch types in the same topology. The turn-on switching loss energy of the 1200 V IGBT decreases compared to a turn-on transition in the 2-level bridge-leg because the commutating diode is only rated for 600 V. Contrary, the 600 V IGBT turn-on loss energy increases as described in [11]. The switching loss energies have been measured with a T-type bridge-leg hardware setup for every switching transition.

In order to calculate the operating point dependent 3LT²C efficiency, an algorithm described in [15] was adopted. It is important that the optimal clamping is considered correctly in order to determine the switching and conduction losses over the phase-angle of the output voltage (cf. Fig. 3). Finally, the average losses in each semiconductor and the efficiency of the 3LT²C can be calculated.

Generally, the 3LT²C obtains very low losses for a wide range of switching frequencies. The conduction losses are comparable with the 2-level converter but the switching losses are further reduced because the commutation voltage is only half of the DC-link voltage $U_\mathrm{dc}/2$. A detailed loss analysis and a comparison with the conventional 2-level and the 3-level NPC converter can be found in [11].

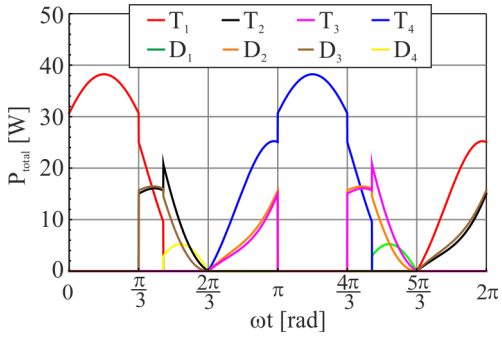

Figure 3: Semiconductor loss distribution over an output voltage period at $\hat{U}_1 = 325\,\mathrm{V}, \hat{I}_1 = 20.5\,\mathrm{A}, \varphi_1 = 30°, f_\mathrm{s} = 6\,\mathrm{kHz}$.

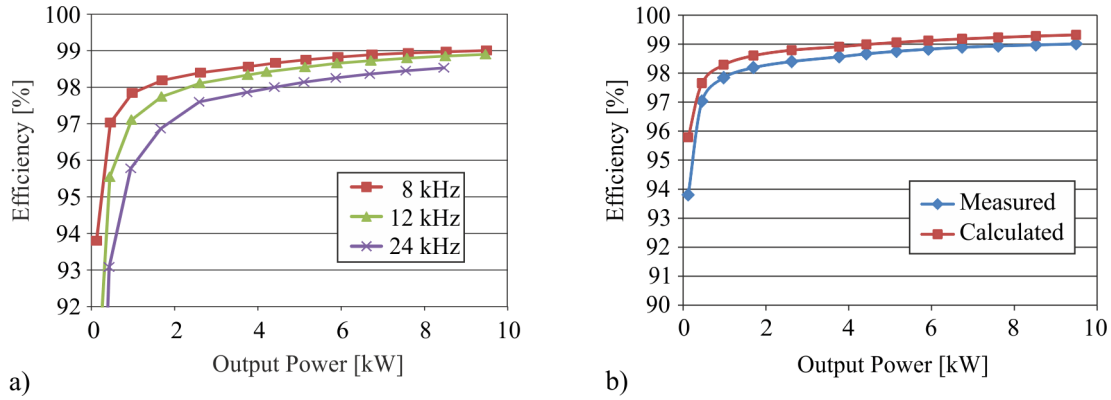

Figure 4: a) Measured efficiency of the 3LT²C prototype supplying a RL-load ($R = 20\,\Omega, L = 2.5\,\mathrm{mH}$). b) Comparison between the calculated and the measured efficiency at $f_\mathrm{s} = 8\,\mathrm{kHz}$.

The efficiency of the 3LT²C has been measured with a Yokogawa WT3000 precision power analyzer (basic power accuracy of 0.02%). The measurements were conducted with a fixed RL-load and the output voltage was increased in small steps. The clamping interval was set to a symmetric clamping around 0° in order to match the small current displacement angle φ_1 resulting from the mainly resistive RL-load. Fig. 4a) shows the measured efficiency over the output power for several switching frequencies. At a switching frequency of 8 kHz the converter reaches the target efficiency of 99 %.

The efficiency calculation resulted in a slightly higher efficiency depicted in Fig. 4b). The deviation can be explained with the approximative linear models of the conduction and switching losses.

In a next step, the converter efficiency in the operating points given by the machine can be calculated. The operating points are dependent on the control of the machine and change with output torque and rotational speed. In the next section, the efficiency optimal control of the induction machine is presented, which has a major impact on the electrical operating point consisting of terminal voltage, current and current displacement angle. The influence on the converter efficiency is presented in section 5.

3 Model-based induction machine efficiency optimization

The induction machine efficiency is highly dependent on the operating point. Conventionally, the machine is controlled with constant rotor flux (corresponding to constant u/f control) and therefore is overmagnetized for most of the operating points with low torque. The related ohmic and iron losses are high and reduce the machine efficiency. To overcome this drawback, several optimized control methods have been proposed over the last decades. Basically they can be divided into search algorithms where a control variable (i.e. the rotor flux) is altered periodically to find the operating point with minimum losses, and model-based optimizers which directly adjust the rotor flux dependent on the operating point.

In this paper a model-based optimizer is implemented which adapts the rotor flux in order to

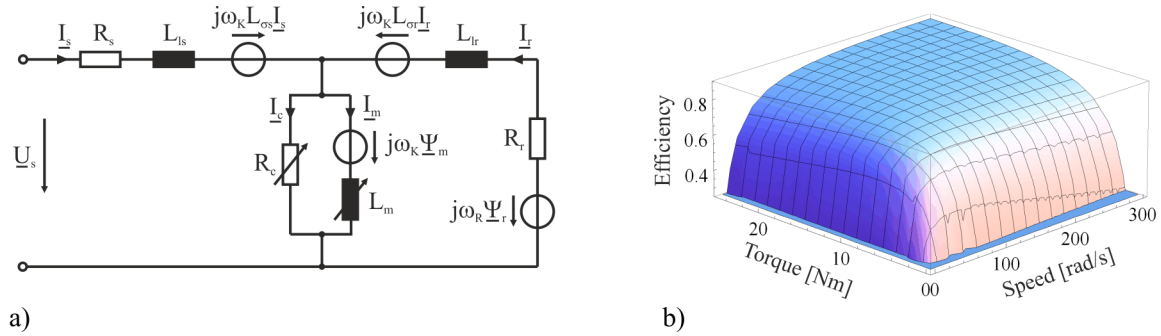

Figure 5: a) Induction machine equivalent circuit. b) Induction machine efficiency with nominal rotor flux over the torque-speed plane.

Table II: Parameters of the induction machine.

Parameter	Variable	Value
Nominal power	P_n	7.5 kW
Nominal efficiency	η_n	89.6 %
Nominal voltage	U_n	230 V
Nominal current	I_n	13.7 A
Nominal torque	T_n	24.7 Nm
Nominal speed	n_n	2900 rpm
Main inductance	L_m	169.6 mH
Stator stray inductance	$L_{\sigma\mathrm{s}}$	3 mH
Rotor stray inductance	$L_{\sigma\mathrm{r}}$	3 mH
Stator resistance	R_s	0.46 Ω
Rotor resistance	R_r	0.41 Ω
Core loss resistance	$R_{\mathrm{c,n}}$	830 Ω
Friction losses	$P_{\mathrm{fric,n}}$	285 W

maximize the machine efficiency. The optimal rotor flux can be derived from the T-equivalent circuit of the induction machine depicted in Fig. 5a) which was shown in [16].

The induction machine considered in this paper is a standard 7.5 kW machine (ecoDrives ACA 132 SB-2/HE) of efficiency class 1. The parameters of the induction machine used for the calculations are summarized in Tab. II. The parameters were determined with standard quasi no-load and blocked rotor tests with a sinusoidal source. The main inductance was determined for rated current. In the following calculations the saturation effects of the main inductance and the leakage inductances are neglected. Also the distinct temperature dependency of parameters such as the rotor and stator resistances is neglected. These simplifications allow to focus on the interactions between the converter and the machine without getting stuck in the complexity of the related topics.

Without loss of generality a rotor flux oriented reference frame can be introduced and the electrical efficiency depending on the torque T_e, the rotor speed ω_R and the rotor flux Ψ_r can be calculated. Fig. 5b) shows the machine efficiency for conventional control with nominal flux. It can be seen that the efficiency drops considerably for low torque and low speed operation.

With some assumptions ($L_{\sigma\mathrm{r}}^2 = 0, R_\mathrm{c} + R_\mathrm{s} = R_\mathrm{c}, R_\mathrm{c} + R_\mathrm{r} = R_\mathrm{c}$) the machine efficiency simplifies to

$$\eta \approx \frac{6L_\mathrm{m}^2\omega_\mathrm{R}p^2\Psi_\mathrm{r}^2R_\mathrm{c}T_\mathrm{e}}{9p^2\Psi_\mathrm{r}^4R_\mathrm{c}R_\mathrm{s} + 8L_{\sigma\mathrm{r}}L_\mathrm{m}R_\mathrm{c}R_\mathrm{s}T_\mathrm{e}^2 + L_\mathrm{m}^2(3\omega_\mathrm{R}p^2\Psi_\mathrm{r}^2 + 2R_\mathrm{c}T_\mathrm{e})(3\omega_\mathrm{R}p^2\Psi_\mathrm{r}^2 + 2(R_\mathrm{r} + R_\mathrm{s})T_\mathrm{e})}. \tag{1}$$

If Eq. 1 is differentiated with respect to the rotor flux and set to zero, the optimal rotor flux maximizing the electrical efficiency can be found according Eq. 2.

$$\Psi_{\mathrm{r,opt}} = \sqrt{\frac{2}{3p}} \cdot \left[\frac{L_\mathrm{m}^2R_\mathrm{c}(R_\mathrm{r} + R_\mathrm{s}) + 2L_\mathrm{m}L_{\sigma\mathrm{r}}R_\mathrm{c}R_\mathrm{s}}{p^2L_\mathrm{m}^2\omega_\mathrm{R}^2 + R_\mathrm{c}R_\mathrm{s}}\right]^{\frac{1}{4}} \cdot \sqrt{T_\mathrm{e}} \tag{2}$$

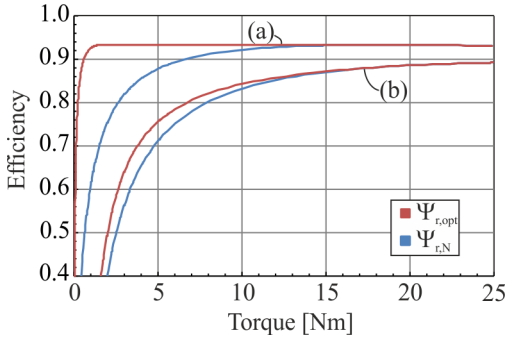

Figure 6: Induction machine efficiency with nominal and optimal rotor flux at nominal speed. a) Pure electrical efficiency, b) friction and windage losses included.

The rotor leakage inductance can be neglected if it is small and the optimal rotor flux reduces to

$$\Psi_{\mathrm{r,opt}} \approx \sqrt{\frac{2}{3p}} \cdot \left[\frac{L_{\mathrm{m}}^2 R_{\mathrm{c}}(R_{\mathrm{r}}+R_{\mathrm{s}})}{p^2 L_{\mathrm{m}}^2 \omega_{\mathrm{R}}^2 + R_{\mathrm{c}} R_{\mathrm{s}}}\right]^{\frac{1}{4}} \cdot \sqrt{T_{\mathrm{e}}}. \tag{3}$$

The equivalent core loss resistance R_{c} is dependent on the electrical frequency. As an approximation it can be scaled linearly with the rotor speed (cf. [17]) because the slip speed is small for controlled inverter operation. A temperature corrected value of the rotor resistance R_{r} could be used for the computation of the optimal flux reference due to its distinct temperature dependency.

The optimal rotor flux usually is lower than the rated flux for low torque operation and higher than the rated value for low speed and high torque operation. The minimum and maximum rotor flux are constrained to 30% and 100% of the rated flux in order to keep a good dynamic response and not to saturate the machine.

The induction machine efficiency can be increased in a wide operating range. Curve set (a) in Fig. 6 shows the achievable pure electric efficiency with the optimal rotor flux. The efficiency can be maintained on a high level also for low torque operation. Unfortunately all conventional machines suffer from additional mechanical losses. The machine efficiency is decreased due to friction and windage. Due to the shaft mounted fan of the self-cooled induction machine these loss components are considerably high ($P_{\mathrm{fric,n}} = 285\,\mathrm{W}$) and can not be neglected. For the machine used in the test bench the mechanical losses have been measured and approximated with a least squares curve fit.

$$P_{\mathrm{fric}} = 0.0283 \cdot \omega_{\mathrm{R}}^{1.613} \tag{4}$$

Curve set (b) in Fig. 6 shows the achievable efficiency including the mechanical losses. It is still possible to increase the efficiency by several percent for low torque operation if the optimal rotor flux is used.

The terminal behavior of the machine changes considerably if operated with the optimal rotor flux. In the low torque region the supplied voltage and the current decrease. Also the voltage to current displacement angle reduces from an inductive behavior to about 40°. This has again an impact on the converter efficiency what is discussed in section 5.

4 Comparison of the harmonic machine losses

The harmonic machine losses due to the pulsed output voltage depend on many manufacturing specific machine parameters such as lamination thickness, winding type, slotting and are difficult to calculate and to measure. Depending on the switching frequency, the harmonic losses consist not only of ohmic but also of iron losses. A promising approach to estimate the influence of different topologies and modulation schemes is the harmonic loss factor curve [18]. Basically, a characteristic loss factor curve is determined by measurement which describes the harmonic losses depending on the supplied voltage frequency spectrum.

In this paper a similar approach was chosen. The harmonic losses of the machine have been measured for several switching frequencies and for 2-level and 3-level modulation. To measure

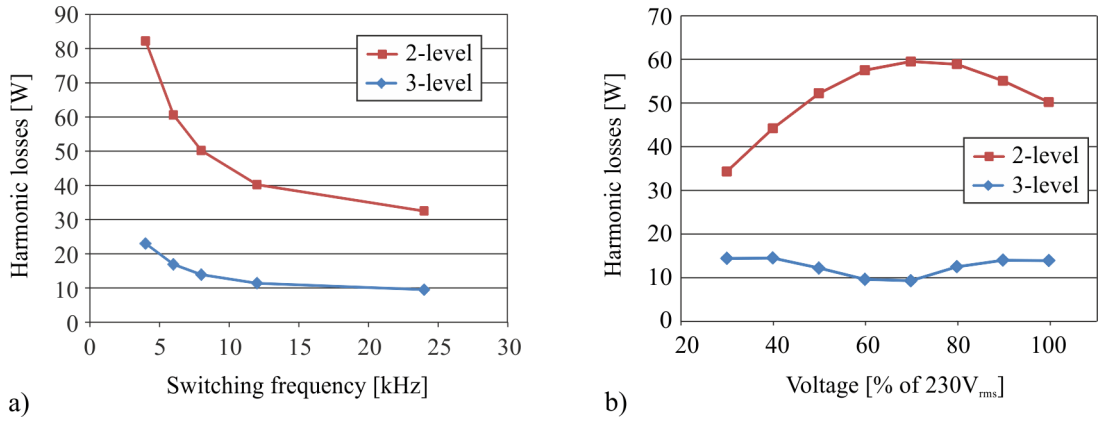

Figure 7: a) Measured harmonic machine losses as a function of the switching frequency ($U_s = 230\,\mathrm{V}$). b) Harmonic machine losses as a function of the output voltage ($f_s = 8\,\mathrm{kHz}$).

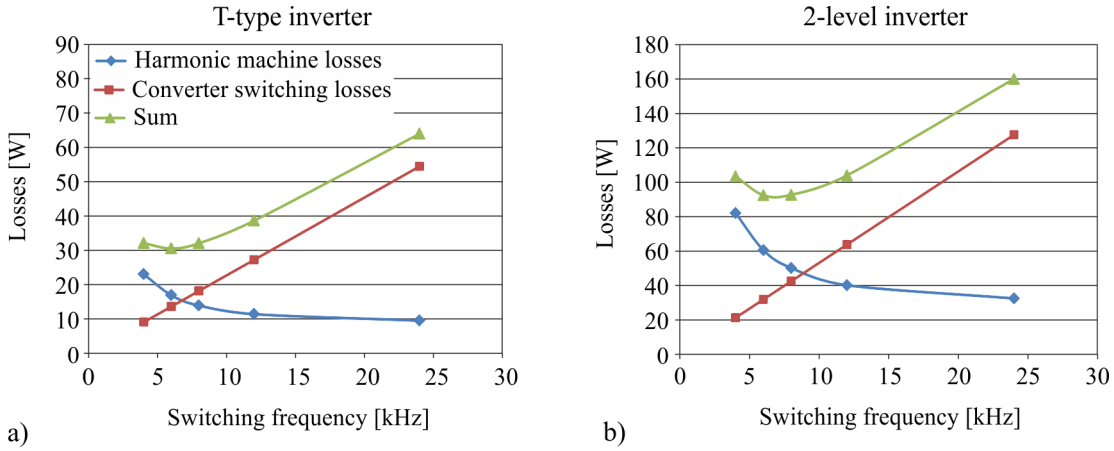

Figure 8: Optimization of the switching frequency dependent loss components with a) the 3LT^{2}C and b) the 2-level converter. The harmonic machine losses are measured during nearly no-load condition and the switching losses are calculated for nominal operation ($f_s = 8\,\mathrm{kHz}$).

the harmonic losses, the precision power analyzer Yokogawa WT3000 was configured in such a way that it automatically subtracts the fundamental active power component from the total measured active power. Therefore, an accurate measurement of the harmonic losses is ensured and no postprocessing is necessary.

The harmonic loss curves for several frequencies and for 2-level and 3-level modulation are depicted in Fig. 7a). The measurements were taken under quasi no-load conditions, therefore only friction and windage losses of the induction machine and the PMSM load machine were applied. It can be seen that the harmonic losses decrease for higher switching frequencies but stagnate on a certain value.

The harmonic machine losses with 3-level modulation are approximately reduced by a factor of 4 compared to the 2-level modulation. This can be explained theoretically with the output voltage spectrum and is analyzed in detail in [19]. There, also the exact relationship between the harmonic losses and the modulation index for 2-level and 3-level modulation is given. The measurements depicted in Fig. 7b) confirm the predictions of [19] precisely. The harmonic losses for 2-level modulation have a maximum at 70% of the rated voltage and the 3-level modulation has two smaller peaks at 30% and 90% of the rated voltage.

5 Total system efficiency

The total system efficiency depends on the converter losses, the fundamental and the harmonic machine losses. The efficiency optimal control of the induction machine takes influence on the converter operating point and also on the harmonic machine losses due to a changed modulation index. The switching frequency has an impact on the converter losses and on the machine har-

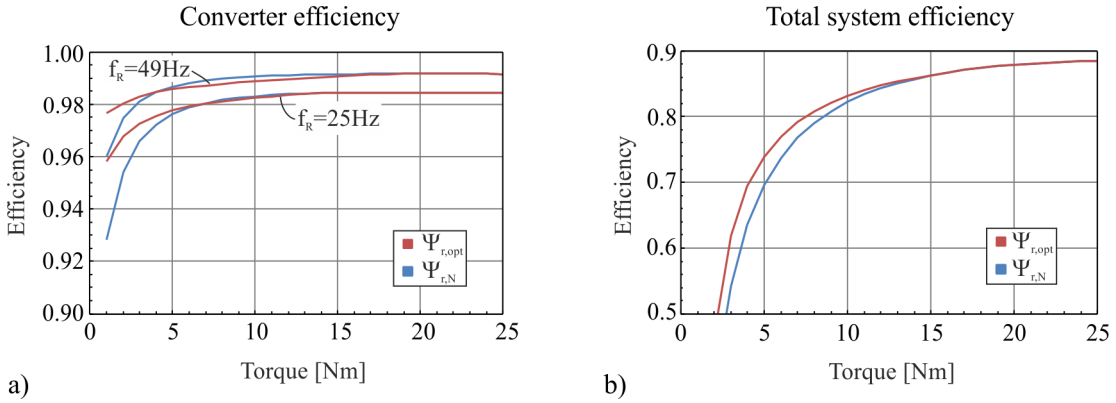

Figure 9: a) Calculated 3LT^{2}C efficiency in the machine operating points for nominal and optimal rotor flux ($f_s = 8\,\text{kHz}$). b) Calculated total drive efficiency including harmonic machine losses ($f_s = 8\,\text{kHz}$).

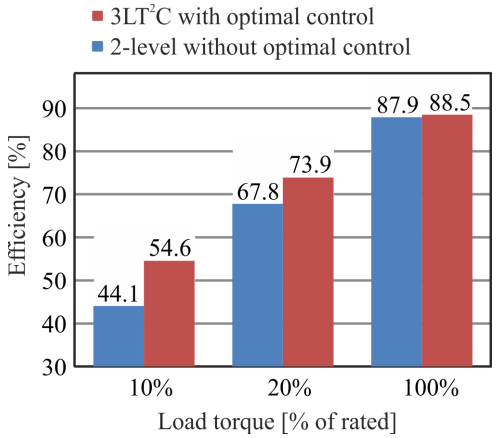

Figure 10: Comparison of the total drive efficiency between a standard 2-level converter with constant rotor flux control and the 3LT^{2}C with optimal rotor flux control ($f_s = 8\,\text{kHz}$).

monic losses. Therefore, a system optimized for efficiency has to consider the optimal switching frequency and the optimal operating point.

In order to find the optimal switching frequency, which results in minimum losses of the total system, the harmonic machine losses, the converter switching losses, and their sum are depicted in Fig. 8a) for the 3LT^{2}C and in Fig. 8b) for the 2-level converter. The switching losses have been calculated for rated speed and torque. The harmonic machine losses have been measured at no-load condition. Although there are some variations of the harmonic machine losses under loaded conditions [10] they are assumed to be small and are neglected. The minimum of the total switching frequency dependent losses is at $f_s = 6\,\text{kHz}$ for the 3LT^{2}C and at $f_s = 7\,\text{kHz}$ for the 2-level converter. A higher switching frequency therefore does not reduce the total losses and should only be chosen if necessary because of the dynamic performance or the acoustic noise reduction.

Although this approach allows no statements for the optimal switching frequency of an arbitrary machine and converter combination the results will potentially be similar for comparable machines and power ratings.

The optimal machine operating point influences the fundamental machine losses and the converter losses. In order to find the global minimum, both subsystems have to be considered and should be optimized at the same time. For low voltage applications, the machine losses are clearly dominant and the optimal operating point achieved by the machine efficiency optimization alone is very close to the total system optimal operating point. It is therefore sufficient to use the optimal rotor flux reference in order to optimize the total system efficiency.

The converter efficiency in the operating points required by the machine is depicted in Fig. 9a) for control with nominal and optimal rotor flux. If the torque is below 20% of rated, the optimal rotor flux has a positive impact on the converter efficiency. This is mainly due to a reduced voltage to current displacement angle. For higher torques, the 3LT^{2}C efficiency is very high and remains in the range from 98% to 99%.

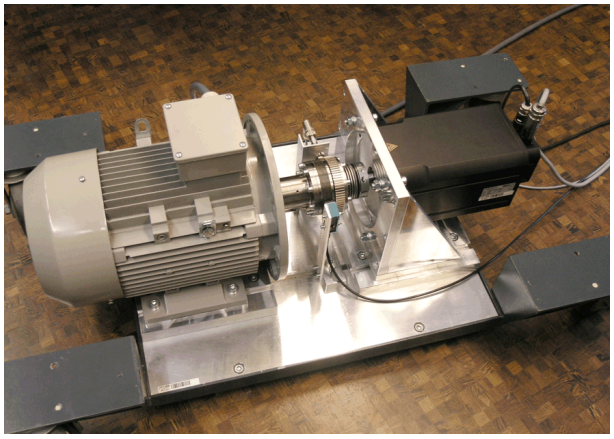

Figure 11: Machine test bench with an induction machine and the PMSM load machine. Torque and speed are measured with a wireless torque transducer (Magtrol TF 210).

The total system efficiency is depicted in Fig. 9b). Due to the very low losses of the 3LT²C the total drive efficiency is mainly determined by the machine. With the optimal rotor flux the efficiency can be increased in the low torque region ($T_e < 20\% \cdot T_n$) by more than 6%. Naturally, the absolute energy savings are considerably lower in this low torque region because the processed power is also decreased. If these absolute losses which can be saved are compared to the nominal machine power an equivalent efficiency increase of approximately 1.2% can be achieved.

Finally, the conventional drive system consisting of a 2-level converter with a standard machine control algorithm (constant u/f) can be compared to the optimized drive system with the new 3LT²C (cf. Fig. 10). In the low torque region ($T_e < 20\% \cdot T_n$) the efficiency can be increased by more than 6% by the use of the optimal flux control and even for rated load, the efficiency can be increased by 0.6% because of the reduced harmonic machine losses and the higher efficiency of the 3LT²C. The machine will obtain only small additional heating by the harmonic losses and the insulation stress is reduced because of the 3-level output voltage waveform.

6 Hardware setup

The measurements have been accomplished with a 99% efficient 10 kW prototype of the 3LT²C depicted in Fig. 1 and a standard 7.5 kW induction machine (ecoDrives ACA 132 SB-2/HE). The induction machine is mounted on a test bench and coupled with a highly precise torque transducer (Magtrol TF 210, 0.05% accuracy) to a PMSM load machine (LST-158-4-30-560) shown in Fig. 11. The losses are measured directly with the high precision power analyzer Yokogawa WT3000. It is able to directly calculate the fundamental and harmonic loss components and therefore no additional post processing is necessary.

7 Conclusion

In this paper a 3-phase 3-level T-type converter topology for high efficiency low voltage drive applications is presented. The drive system is competitive to standard 2-level solutions because of the relatively low cost 3LT²C. The total system efficiency is optimized considering fundamental and harmonic losses in the converter and in the machine. A total efficiency increase of more than 6% in the low torque range was achieved. The proposed variable speed drive is tested with a hardware prototype and a machine test bench including high precision power and torque measurements.

Employing new semiconductor devices such as SiC-diodes will not lead to a significant efficiency increase of the total drive system because the harmonic machine losses and the switching losses are already on a very low level with the 3LT²C. The only way to further increase the total drive efficiency is reducing the conduction losses of the switches or reducing the mechanical, ohmic and iron losses of the machine.

References

[1] J. K. Steinke, "Grundlagen für die Entwicklung eines Steuerverfahrens für GTO-Dreipunktwechselrichter für Traktionsantriebe," in *etzArchiv*, vol. 10, pp. 215–220, VDE-Verlag, Berlin, Germany, 1988.

[2] R. Joetten, M. Gekeler, and J. Eibel, "AC drive with three-level voltage source inverter and high dynamic performance microprocessor control," in *Proc. of the European Conf. on Power Electronics and Applications, EPE 85*, (Bruxelles, Belgium), pp. 3.1–3.6, October 1985.

[3] B. Fuld, "Aufwandsarmer Thyristor-Dreistufen-Wechselrichter mit geringen Verlusten," in *etzArchiv*, vol. 11, pp. 261–264, VDE-Verlag, Berlin, Germany, 1989.

[4] T. Takeshita and N. Matsui, "PWM control and input characteristics of three-phase multi-level AC/DC converter," in *Proc. of the 23rd Annual IEEE Power Electronics Specialists Conf. PESC 92*, pp. 175–180, 1992.

[5] R. Teichmann and S. Bernet, "A comparison of three-level converters versus two-level converters for low-voltage drives, traction, and utility applications," *IEEE Transactions on Industry Applications*, vol. 41, pp. 855–865, May–June 2005.

[6] J. Ewanchuk, J. Salmon, and A. M. Knight, "Performance of a high-speed motor drive system using a novel multilevel inverter topology," *IEEE Transactions on Industry Applications*, vol. 45, no. 5, pp. 1706–1714, 2009.

[7] J. M. Moreno-Eguilaz, M. Cipolla, and J. Peracaula, "Induction motor drives energy optimization in steady and transient states: a new approach," in *Proc. of the European Conf. on Power Electronics and Applications, EPE 97*, pp. 3705–3710, 1997.

[8] K. S. Rasmussen and P. Thogersen, "Model based energy optimiser for vector controlled induction motor drives," in *Proc. of the European Conf. on Power Electronics and Applications, EPE 97*, pp. 3711–3716, 1997.

[9] A. Boglietti, A. Cavagnino, and A. M. Knight, "Isolating the impact of PWM modulation on motor iron losses," in *Proc. of the IEEE Industry Applications Society Annual Meeting, IAS 08*, pp. 1–7, 2008.

[10] A. Boglietti, A. Cavagnino, A. M. Knight, and Y. Zhan, "Factors affecting losses in induction motors with non-sinusoidal supply," in *Proc. of the IEEE Industry Applications Society Annual Meeting, IAS 07*, pp. 1193–1199, 2007.

[11] M. Schweizer, I. Lizama, T. Friedli, and J. W. Kolar, "Comparison of the chip area usage of 2-level and 3-level voltage source converter topologies," in *Proc. of the 36th Annual Conf. of the IEEE Industrial Electronics Society, IECON 2010*, 2010.

[12] J. W. Kolar, H. Ertl, and F. C. Zach, "Influence of the modulation method on the conduction and switching losses of a PWM converter system," *IEEE Transactions on Industry Applications*, vol. 27, no. 6, pp. 1063–1075, 1991.

[13] B. Kaku, I. Miyashita, and S. Sone, "Switching loss minimised space vector PWM method for IGBT three-level inverter," *IEE Proc. of Electric Power Applications*, vol. 144, pp. 182–190, May 1997.

[14] J. Pou, D. Boroyevich, and R. Pindado, "New feedforward space-vector PWM method to obtain balanced AC output voltages in a three-level neutral-point-clamped converter," *IEEE Transactions on Industrial Electronics*, vol. 49, no. 5, pp. 1026–1034, 2002.

[15] M. Schweizer, T. Friedli, and J. W. Kolar, "Comparison and implementation of a 3-level NPC voltage link back-to-back converter with SiC and Si diodes," in *Proc. of the 25th Annual IEEE Applied Power Electronics Conf. and Exposition, APEC 2010*, pp. 1527–1533, 2010.

[16] K. Matsuse, T. Yoshizumi, S. Katsuta, and S. Taniguchi, "High-response flux control of direct-field-oriented induction motor with high efficiency taking core loss into account," *IEEE Transactions on Industry Applications*, vol. 35, no. 1, pp. 62–69, 1999.

[17] A. Dittrich, "Model based identification of the iron loss resistance of an induction machine," in *Proc. of the 7th Int. Power Electronics and Variable Speed Drives Conf.*, pp. 500–503, 1998.

[18] K. Bradley, W. Cao, J. Clare, and P. Wheeler, "Predicting inverter-induced harmonic loss by improved harmonic injection," *IEEE Transactions on Power Electronics*, vol. 23, no. 5, pp. 2619–2624, 2008.

[19] A. Ruderman and B. Reznikov, "PWM power converter voltage quality bounds and their applicability to non-pwm control schemes," in *Proc. of the 12th Int. Optimization of Electrical and Electronic Equipment Conf., OPTIM*, pp. 618–624, 2010.